Accurate Analytical Multiple-Access Performance of Time-Hopping Biorthogonal PPM IR-UWB Systems

Marijan HERCEG, Ratko GRBIĆ, Tomislav ŠVEDEK
Faculty of Electrical Engineering, University of Osijek, Trpimirova 2B, 31000 Osijek, Croatia
marijan.herceg@etfos.hr, ratko.grbic@etfos.hr, tomislav.svedek@etfos.hr

***Abstract*—In this paper, the characteristic function (CF) method is used to derive the symbol error rate (SER) expression for time-hopping impulse radio ultra–wideband (TH-IR-UWB) systems with a biorthogonal pulse position modulation (BPPM) scheme in the presence of a multi-user interference (MUI). The derived expression is validated with the Monte-Carlo simulation and compared with orthogonal PPM. Moreover, the analytical results are compared with the Gaussian approximation (GA) of MUI which is shown to be inaccurate for a medium and large signal-to-noise ratio (SNR). It is also shown that the BPPM scheme outperforms the PPM scheme for all SNR. At the end, the influence of different system parameters on the BPPM performance is analyzed.**

***Index Terms*—symbol error rate, biorthogonal pulse position modulation, characteristic function, ultra-wideband, multi-user interference.**

I. INTRODUCTION

Trends in modern communication systems place high demands on low power consumption, high speed transmission and anti-interference characteristics. Therefore impulse radio ultra–wideband (IR-UWB) [1] radio systems have recently gained an increase in popularity. Since IR-UWB symbols are transmitted with short pulses (< 2 ns), in IR-UWB systems, energy has been spread over the frequency bands of up to 10 GHz. In order to flatten out the power spectrum density of the IR-UWB signals and to reduce narrowband interference some extra coding techniques are applied in [2]. State-of-the-art IR-UWB systems present many applicable modulation methods like the Pulse Amplitude Modulation (PAM), PPM, Pulse Shape Modulation (PSM), on-off-keying (OOK), binary phase-shift keying (BPSK) and Pulse Interval Modulation (PIM) [3]. Many combined hybrid techniques for IR-UWB communication systems have been applied recently, such as the Pulse Position Amplitude Modulation (PPAM) [4], OOK-PSM [5], and hybrid Shape-Amplitude Modulation [6]. Since the first time that multiple-access TH-UWB systems were presented [1] lots of research has been done in order to analyze the multi-user interference (MUI) performance over additive white Gaussian noise (AWGN). The most common method used for representing MUI is Gaussian approximation (GA) [7], while in [8], it is shown that the GA method is not accurate for a medium and large signal-to-noise ratio.

An analytical method for calculating BER for TH-PPM, TH-BPSK UWB systems based on CF is presented in [9], and later extended on N - orthogonal PPM in [10].

This work was supported by the Ministry of Science, Education and Sports, Republic of Croatia, through Research Grants 165-0361630-3049 and 165-0361621-2000.

Digital Object Identifier 10.4316/AECE.2011.02010

In this paper we extend the CF analysis on the biorthogonal pulse position modulation (BPPM) scheme which was first presented in [11]. In BPPM a signal set is formed using 2^k orthogonal PPM signals and including their antipodal version which overall forms a set of $N = 2^{k+1}$ symbols (N–ary BPPM).

This paper is organized as follows: Section 2 describes the TH-IR-UWB BPPM system model. In Section 3 the accurate analytical expression for BPPM error probability is derived. The numerical results are given in Section 4 while some conclusions are given in Section 5.

II. TH-IR-UWB BPPM SYSTEM MODEL

The asynchronous BPPM TH-IR-UWB system is described in detail in [11]. A typical N–ary BPPM signal for k-th user can be written as

$$s^{(k)} = \sum_{l=-\infty}^{\infty} \sum_{j=lN_s}^{(l+1)N_s-1} b_l^{(k)} \sqrt{\frac{E_s}{N_s}} p(t - jT_f - c_j^{(k)}T_c - d_l^{(k)}\delta), \tag{1}$$

where E_s is the energy per symbol, N_s is the number of pulses used to transmit a single symbol, l is the symbol index, $p(t)$ is the signal pulse waveform with duration T_p and normalized energy $\int_{-\infty}^{\infty} p^2(t)dt = 1$. T_f is the frame duration thus defining symbol duration as $T_s = N_s T_f$. $\left\{c_j^{(k)}\right\}$ is the pulse shift pattern also called the TH sequence of k-th user which is pseudorandom and each element assumes any value from $0 \le c_j^{(k)} \le N_h - 1$. T_c is the chip duration and satisfies $N_h T_c < T_f$. δ is the time shift parameter and it is set to be $>T_p$ which provides orthogonality between pulse positions within the symbol. $d_l^{(k)} \in \{0,...,N/2-1\}, b_l^{(k)} \in \{1,-1\}$ is determined by the l-th data symbol of the k-th source and thus represents the position and the amplitude level of the pulse in the N–ary BPPM symbol, respectively.

In our work we have assumed, without the loss of generality, that:

- User 1 is the desired user and other $N_u - 1$ users are the interference.
- TH code for first user is $c_j^{(1)} = 0, \forall j$.
- $d_0^{(1)}$ and $b_0^{(1)}$ are transmitted.
- Perfect code synchronization at the receiver and power control $A_k = 1$.

If AWGN channel model is used, the signal received in the multi-user environment is given as

$$r(t)=\sum_{k=1}^{N_u} A_k s^{(k)}(t-\tau_k)+n(t), \tag{2}$$

where N_u is the number of users, τ_k is the time delay of the k-th user, A_k is the channel attenuation for k-th user and $n(t)$ is the additive white Gaussian noise with two sided power spectral density $N_0/2$.

In order to demodulate the received signal it is assumed that the correlator based receiver shown on Fig. 1 is used.

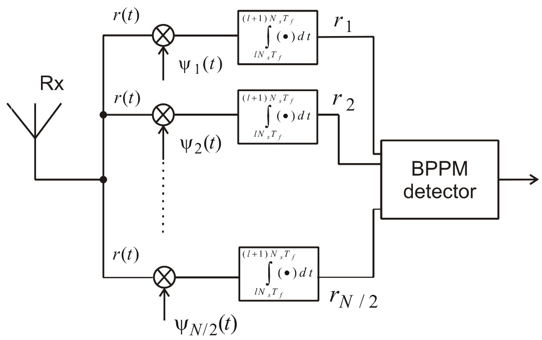

Figure 1. BPPM receiver

As it can be seen from Fig. 1 the BPPM receiver in i-th branch correlates the received signal with the template waveform which is given for the first user as

$$\psi_i^{(1)}(t)=\sum_{j=0}^{N_s}\sqrt{\frac{N_s}{E_s}}\,p(t-jT_f-c_j^{(1)}T_c-(i-1)\delta-\tau_1), \quad . \tag{3}$$
$$i=1,...N/2.$$

In our work we have assumed that the pulse shape used for data transmission (also the template pulse) is the second derivative of the Gaussian pulse given in [9]

$$p(t)=\left[1-4\pi\left(\frac{t}{\tau_p}\right)^2\right]\exp-\left[2\pi\left(\frac{t}{\tau_p}\right)^2\right], \tag{4}$$

where τ_p is the time normalization factor. Defining autocorrelation function of $p(t)$ as

$$R(x)=\int_{-\infty}^{\infty} p(t)p(t-x)dt, \tag{5}$$

we can then write $R(x)$ as

$$R(x)=\left[1-4\pi\left(\frac{x}{\tau_p}\right)^2+\frac{4\pi^2}{3}\left(\frac{x}{\tau_p}\right)^4\right]\exp\left[-\pi\left(\frac{x}{\tau_p}\right)^2\right]. \tag{6}$$

III. Performance Analysis

In order to derive the symbol error rate (SER) expression of the BPPM TH-IR-UWB system we have assumed that the first user is the desired one and that the 0-th transmitted information symbol is sent and that it is equal to $d_0^{(1)}=0, b_0^{(1)}=1$. Using the receiver shown on Fig. 1 we can define the correlators output with vector $\mathbf{r}=[r_1\ r_2\ .....\ r_{N/2}]$, where r_i is

$$r_i=\sum_{j=0}^{N_s-1}\int_{jT_f}^{(j+1)T_f} r(t)\psi_i^{(1)}(t)dt=\begin{cases}S+I_i+N_i, & i=1\\ I_i+N_i, & i=1,...,N/2.\end{cases} \tag{7}$$

$S=N_sR(0)$ is the contribution of the desired transmitted information symbol $d_0^{(1)}, b_0^{(1)}$ to the decision statistic r_1. N_i is the AWGN component at the output of i-th correlator modeled as a Gaussian random variable with zero mean and variance $\sigma_n^2=N_s^2R(0)/2(E_s/N_0)$. I_i is MUI component at the output of i-th correlator and it is given as

$$I_i=\sum_{k=2}^{N_u}\int_0^{N_sT_f} s^{(k)}(t-\tau_k)\psi_i^{(1)}(t)dt\,. \tag{8}$$

From [11], [12] it can be seen that the BPPM detector decides which symbol is sent in favor of r_i with the largest magnitude, and then the sign of that magnitude is used to decide which one of the two possible amplitude levels is sent. Overall probability of the symbol error, conditioned on $d_0^{(1)}=0, b_0^{(1)}=1$, can then be calculated using

$$P_{e\_BPPM}=1-\int_0^{\infty} P(\bigcap_{i=2}^{N/2}|r_i|<r_1)|\,d_0^{(1)}=0,b_0^{(1)}=1)p(r_1)dr_1\,. \tag{9}$$

Following the same procedure as in [12] we will first derive the probability that

$$P(\bigcap_{i=2}^{N/2}|I_i+N_i|<r_1)=P(\bigcap_{i=2}^{N/2}-r_1<I_i+N_i<r_1)\,. \tag{10}$$

To derive the probability that $P(-r_1<I_i+N_i<r_1)$ using the CF method we will write I_i as

$$\begin{aligned} I_i=&\sum_{k=2}^{N_u}\sum_{j=0}^{N_s-1}\sum_{j'=-\infty}^{\infty}\int_{-\infty}^{\infty} b^{(k)}_{\lfloor j'/N_s\rfloor}x\\ &xp(t-j'T_f-c_{j'}^{(k)}T_c-d^{(k)}_{\lfloor j'/N_s\rfloor}\delta-\tau_k)x\\ &xp(t-jT_f-(i-1)\delta-\tau_1)dt=\\ =&\sum_{k=2}^{N_u}\sum_{j=0}^{N_s-1}\sum_{j'=-\infty}^{\infty} b^{(k)}_{\lfloor j'/N_s\rfloor}\mathrm{x}\\ &xR((j'-j)T_f+c_{j'}^{(k)}T_c+(d^{(k)}_{\lfloor j'/N_s\rfloor}-(i-1))\delta+(\tau_k-\tau_1)) \end{aligned} \tag{11}$$

Due to the property that $R(x)$ is nonzero only for $|x|<T_p$ and assuming that [7]

$$N_hT_c<T_f/2-2T_p\,, \tag{12}$$

we may assume that only one pulse from each interfering user in each frame contributes to the MUI which implies that $j'=j$. The difference between time arrivals of user one and user k can be modeled as [7]

$$\tau_k-\tau_1=j_kT_f+\alpha_k, \quad -\frac{T_f}{2}\le\alpha_k<\frac{T_f}{2}, \tag{13}$$

where j_k is the time difference between $\tau_k-\tau_1$ rounded to the nearest integer and α_k is the error in the rounding process which is modeled as a random variable uniformly distributed over the interval [$-T_f/2$, $T_f/2$]. Then (11) can be rewritten as

$$I_i=\sum_{k=2}^{N_u}\sum_{j=0}^{N_s-1} b^{(k)}_{\lfloor (j+j_k)/N_s\rfloor}R_i(d^{(k)}_{\lfloor (j+j_k)/N_s\rfloor}\delta+c_j^{(k)}T_c+\alpha_k), \tag{14}$$

where

$$R_i(x)=R(x-(i-1)\delta)\,. \tag{15}$$

The interfering signal $d^{(k)}_{\lfloor (j+j_k)/N_s\rfloor}, b^{(k)}_{\lfloor (j+j_k)/N_s\rfloor}$ may change value during transmission of symbol 0 so we can rewrite (14) as

$$I_i = \sum_{k=2}^{N_u} I_i^{(k)}, \tag{16}$$

where

$$I_i^{(k)} = \left(\sum_{j=0}^{\gamma_k - 1} b_0^{(k)} R_i(\Delta t_{0,j}^{(k)}) + \sum_{j=\gamma_k}^{N_s-1} b_1^{(k)} R_i(\Delta t_{1,j}^{(k)}) \right), \tag{17}$$

with

$$\begin{aligned} \Delta t_{0,j}^{(k)} &= d_0^{(k)}\delta + c_j^{(k)} T_c + \alpha_k, \\ \Delta t_{1,j}^{(k)} &= d_1^{(k)}\delta + c_j^{(k)} T_c + \alpha_k. \end{aligned} \tag{18}$$

Subscript 0 and 1 represent two neighbor symbols of the *k*-th user that overlap with the transmission time of the first user symbol 0, γ_k is a random variable uniformly distributed over [0, N_s - 1]. If we wrote

$$I_i^{(k)} = X_i^{(k)} + Y_i^{(k)}, \tag{19}$$

where

$$X_i^{(k)} = \sum_{j=0}^{\gamma_k - 1} b_0^{(k)} R_i(t_{0,j}^{(k)}), \tag{20}$$

$$Y_i^{(k)} = \sum_{j=\gamma_k}^{N_s-1} b_1^{(k)} R_i(t_{1,j}^{(k)}), \tag{21}$$

then CF of $X_i^{(k)}$ conditioned on $d_0^{(k)}, b_0^{(k)}, \alpha_k$ and γ_k is

$$\begin{aligned} &\phi_{X_i^{(k)}|d,b,\alpha,\gamma}(\omega) = \\ &E\left[\exp(j\omega \sum_{j=0}^{\gamma_k-1} b_0^{(k)} R_i(\Delta t_{0,j}^{(k)})) \,|\, d_0^{(k)} = d, b_0^{(k)} = b, \alpha_k = \alpha, \gamma_k = \gamma \right] = \\ &\left(\frac{1}{N_h} \sum_{h=0}^{N_h-1} \exp(j\omega b R_i(d\delta + hT_c + \alpha)) \right)^{\gamma}, \end{aligned} \tag{22}$$

where E[*] is the mean value operator. The upper expression comes from the fact that $c_j^{(k)}$ can have any value in $\{0,1,...,N_h-1\}$ with equal probability. Assuming that all symbols are equally likely and using the theorem of total probability we can write

$$\begin{aligned} \phi_{X_i^{(k)}|\alpha,\gamma}(\omega) = \frac{1}{NN_h^{\gamma}} \sum_{m=0}^{N/2-1} \Bigg[\left(\sum_{h=0}^{N_h-1} \exp(j\omega R_i(m\delta + hT_c + \alpha)) \right)^{\gamma} + \\ + \left(\sum_{h=0}^{N_h-1} \exp(-j\omega R_i(m\delta + hT_c + \alpha)) \right)^{\gamma} \Bigg]. \end{aligned} \tag{23}$$

Using the same procedure the CF of $Y_i^{(k)}$ is

$$\begin{aligned} \phi_{Y_i^{(k)}|\alpha,\gamma}(\omega) = \frac{1}{NN_h^{N_s-\gamma}} \sum_{m=0}^{N/2-1} \Bigg[\left(\sum_{h=0}^{N_h-1} \exp(j\omega R_i(m\delta + hT_c + \alpha)) \right)^{N_s-\gamma} + \\ + \left(\sum_{h=0}^{N_h-1} \exp(-j\omega R_i(m\delta + hT_c + \alpha)) \right)^{N_s-\gamma} \Bigg]. \end{aligned} \tag{24}$$

Assuming that the data sequence of the *k*-th user and each user chip sequence is independent we may write the CF of $I_i^{(k)}$ as

$$\phi_{I_i^{(k)}|\alpha,\gamma}(\omega) = \phi_{X_i^{(k)}|\alpha,\gamma}(\omega)\phi_{Y_i^{(k)}|\alpha,\gamma}(\omega). \tag{25}$$

After further averaging of $\phi_{I_i^{(k)}|\alpha,\gamma}(\omega)$ over α and γ we may write

$$\phi_{I_i^{(k)}}(\omega) = \frac{1}{N_s T_f} \int_{-T_f/2}^{T_f/2} \sum_{n=0}^{N_s-1} \phi_{I_i^{(k)}|\alpha,n}(\omega) d\alpha. \tag{26}$$

At the end the total MUI of ($N_u - 1$) independent users can be written as

$$\phi_{I_i}(\omega) = \prod_{k=2}^{N_u} \phi_{I_i^{(k)}}(\omega). \tag{27}$$

The CF of the N_i is

$$\phi_{N_i}(\omega) = \exp(-\omega^2 \sigma_n^2 / 2). \tag{28}$$

Using the independence of MUI and AWGN we may write the conditional probability by applying the relationship between the CF and the cumulative density function (CDF) of a random variable as [9]

$$F_i(\lambda) = \frac{1}{2} + \frac{1}{\pi} \int_0^{\infty} \frac{\sin(\lambda\omega)}{\omega} \phi_{\Lambda_i}(\omega) d\omega, \tag{29}$$

where

$$\phi_{\Lambda_i}(\omega) = \phi_{I_i}(\omega)\phi_{N_i}(\omega). \tag{30}$$

At the end we may write

$$P(\bigcap_{i=2}^{N/2} -r_1 < I_i + N_i < r_1) = \prod_{i=2}^{N/2} (F_i(r_1) - F_i(-r_1)). \tag{31}$$

From (9), it can be seen that in order to obtain an accurate error performance of BPPM, the probability density function (PDF) of r_1 has to be derived. The r_1 is defined as $r_1 = N_s R(0) + I_1 + N_1$, where I_1 is modeled as a random variable with CF given as (27), while $N_s R(0) + N_1$ can be modeled as a Gaussian random variable with the mean $N_s R(0)$ and variance σ_n^2, and its CF is given as

$$\phi_{N_1}(\omega) = \exp(iN_s R(0)\omega - \omega^2 \sigma_n^2 / 2). \tag{32}$$

Using the inverse fourier transform the PDF of r_1 can be obtained as

$$p(r_1) = \frac{1}{2\pi} \int_{-\infty}^{\infty} \phi_{N_1}(\omega)\phi_{I_1}(\omega) \exp(-i\omega r_1) dr_1. \tag{33}$$

IV. NUMERICAL RESULTS

All numerical results in this paper are obtained using Matlab, with the Monte Carlo simulation being used to validate results.

In Fig 2. accurate analytical SER with GA and Monte Carlo simulation for BPPM with N = 4 for N_s = 2,4 is compared. It can be seen that the GA approximates SER well for a lower signal-to-noise ratio (SNR), while for higher SNR values (>6 dB) the disagreement is very high. It is the result of the fact that for smaller SNR values AWGN is dominant, while for larger SNR values MUI is dominant and thus MUI cannot be approximated well with GA. Also as expected, with the increase of N_s ,SER performance increases significantly.

In Fig 3. BPPM with a different modulation level N for the same bit rate, which is set to 20 Mbps, is compared. It can be seen that BPPM with N = 16 has the best SER performance for smaller SNR values, while BPPM with N = 4 and 8 has better SER performance for higher SNR values.

It comes from the fact that in order to satisfy a condition (12) for the fixed bit rate, due to the longer chip time, BPPM with a higher modulation level has a smaller N_h value, which is an important parameter for decreasing MUI.

Fig 4. shows dependence of the SER performance on a number of users N_u for different modulation levels and bit rate of 20 Mbps. The BPPM with N = 16 performs worst due to the fact that N_h is the smaller value.

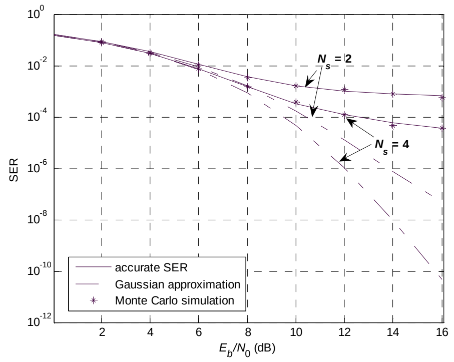

Figure 2. Accurate analytical SER of BPPM versus E_b/N_0 with system parameters $N = 4$, N_s = 2,4, T_f = 50 ns, T_c =N/2*0,9 ns, N_h = 8, τ_p = 0,2877 ns, δ = 0,72 ns, N_u = 8

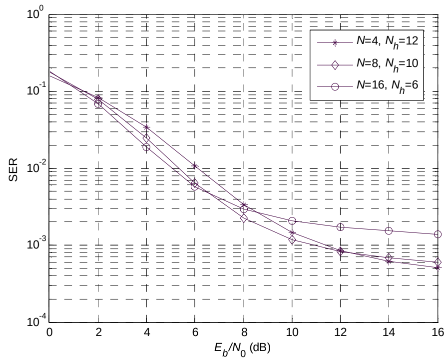

Figure 3. Comparison of BPPM with a different modulation level versus E_b/N_0 for a fixed bit rate (20 Mbps). System parameters are N_s = 2, T_c =N/2*0,9 ns, τ_p = 0,2877 ns, δ = 0,72 ns, N_u = 8

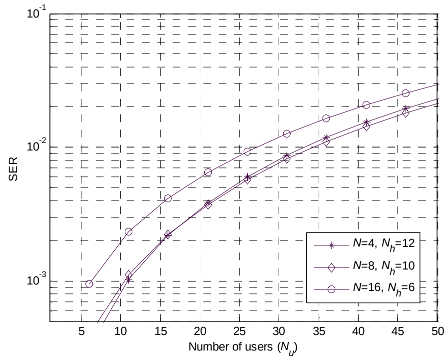

Figure 4. Comparison of BPPM with a different modulation level versus N_u for a fixed bit rate (20 Mbps). System parameters are N_s = 2, T_c =N/2*0,9 ns, τ_p = 0,2877 ns, δ = 0,72 ns, SNR = 15 dB

Finally we compared orthogonal PPM and BPPM with N = 8 for a fixed bit rate in Fig 5. It can be seen that BPPM outperforms PPM for all SNR values. For example, for SNR = 16 dB SER of BPPM is $6*10^{-4}$ while SER of PPM is $1{,}8*10^{-3}$ for N_s = 2 and for N_s = 4 SER is $3*10^{-4}$ and $2{,}8*10^{-3}$, respectively, which are significantly better results.

V. Conclusion

In this paper, an accurate analytical expression for average SER is derived for BPPM TH-IR-UWB systems under MUI and compared with GA and the Monte Carlo simulation.

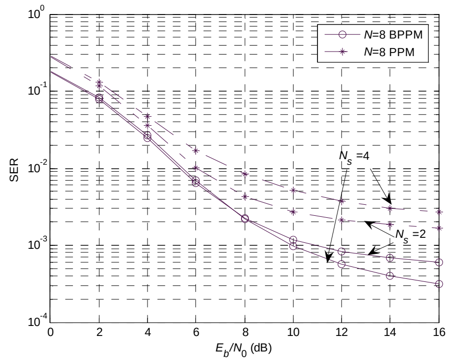

Figure 5. Comparison of BPPM and PPM with a different modulation level versus E_b/N_0 for a fixed bit rate (20 Mbps). System parameters are, T_c =N/2*0,9 ns (N*0,9 ns for PPM), τ_p = 0,2877 ns, δ = 0,72 ns, N_u = 8, for N_s = 2, N_h = 10 (5 for PPM) and for N_s = 4, N_h = 5 (2 for PPM)

It is shown that GA is accurate for small SNR values, while for larger values it significantly underestimates modulation performance. The BPPM scheme is also compared with the PPM scheme where it can be seen that BPPM has a better performance than PPM with half hardware complexity (less correlators). Due to this property the BPPM scheme is attractive for TH-IR-UWB communication systems.

References

[1] R. A. Scholtz, „Multiple access with time-hopping impulse modulation“, Proc. IEEE Military Commun. Conf., pp. 11-14, October. 1993.

[2] T. N. Durnea, N. D. Alexandru, "Calculus of the Power Spectral Density of Ultra Wide Band Pulse Position Modulation Signals Coded with Totally Flipped Code," Advances in Electrical and Computer Engineering, vol. 9, no. 1, pp. 16-21, 2009. [Online]. Available: http://dx.doi.org/10.4316/AECE.2009.010

[3] M. Herceg, T. Švedek, and T. Matić, "Pulse Interval Modulation for Ultra-High Speed IR-UWB Communications Systems," EURASIP Journal on Advances in Signal Processing, vol. 2010, Article ID 658451, 8 pages, 2010. doi:10.1155/2010/658451

[4] H. Zhang, W. Li, and T. A. Gulliver, "Pulse Position Amplitude Modulation for Time-Hopping Multiple-Access UWB Communicatios", IEEE Trans. on Comm., vol. 53, no. 8, August 2005.

[5] S. Majhi and A. S. Madhukumar, "Combining OOK with PSM Modulation for TH-UWB Radio Systems: A Performance Analysis", EURASIP Journal on Wireless Comm. and Networking, vol. 2008.

[6] M. Herceg, T. Matic and T. Svedek, "Performances of hybrid Amplitude Shape Modulation for UWB communications systems over AWGN channel in the single and multi-user environment“, Radioengineering Journal, September 2009.

[7] M. Z. Win and R. A. Scholtz, "Ultra-wide bandwidth time-hopping spread-spectrum impulse radio for wireless multiple-access communications," IEEE Trans. Commun., vol. 48, pp. 679–689, 2000.

[8] G. Durisi and G. Romano, "On the validity of Gaussian approximation to characterize the multiuser capacity of UWB TH PPM," in Proc. IEEE Conf. Ultra Wide-band Systems and Technologies, Baltimore, USA, May 2002, pp. 157–161.

[9] H. Bo and N. C. Beaulieu, "Accurate evaluation of multiple-access performance in TH-PPM and TH-BPSK UWB systems," IEEE Trans. Commun., vol. 52, no. 10, pp. 1758–1766, 2004.

[10] Q. F. Zhou and F. C. M. Lau, "Analytical Performance of M-ary Time-Hopping Orthogonal PPM UWB Systems under Multiple Acces Interference", IEEE Trans. Commun., vol. 56, no. 11, pp. 1780–1784, 2008.

[11] H. Zhang, and T. A. Gulliver, "Biorthogonal Pulse Position Modulation for Time-Hopping Multiple-Access UWB Communicatios", IEEE Trans. On Wireless Comm., vol. 4, no. 3, May 2005.

[12] J. G. Proakis, "Digital Communications", 4th ed., New York: McGraw-Hill, 2001